

Evaluation of Neutron Flux in Boron Neutron Capture Therapy for a 10-Year-Old Child with Head and Neck Rhabdomyosarcoma Using Monte Carlo Simulation

F. M. Salim, E. Hidayanto, W. Setiabudi, F. Arianto*

Department of Physics, Faculty of Science and Mathematics, Diponegoro University, Semarang 1269, Indonesia.

ARTICLE INFO

Article history:

Received 22 May 2025

Received in revised form 9 September 2025

Accepted 11 September 2025

Keywords:

BNCT

Flux neutron

Head and neck rhabdomyosarcoma

Monte carlo

MCNP 6.2

ABSTRACT

Head and neck rhabdomyosarcoma is among the most frequently encountered malignancies in children under the age of 10, necessitating effective treatment modalities with minimal toxicity. Boron Neutron Capture Therapy (BNCT) is recognized as a promising therapeutic alternative in radiotherapy owing to its ability to selectively target malignant cells. The aim of this study was to evaluate the neutron beam quality of a BNCT collimator in a simulation model for the treatment of head and neck rhabdomyosarcoma in a 10-year-old pediatric phantom, using the MCNP 6.2 Monte Carlo method. The simulation included tumor modeling incorporating Gross Tumor Volume (GTV), Clinical Target Volume (CTV), and Planning Target Volume (PTV) to assess neutron flux distribution. The results showed a thermal neutron flux of $5.22 \times 10^9 \text{ n cm}^{-2} \text{ s}^{-1}$, an epithermal neutron flux of $1.22 \times 10^{10} \text{ n cm}^{-2} \text{ s}^{-1}$, and a fast neutron flux of $5.91 \times 10^7 \text{ n cm}^{-2} \text{ s}^{-1}$. Further analysis indicated that the produced epithermal flux exceeded the minimum standard recommended by the IAEA, and the highest flux was concentrated in the GTV region, suggesting effective tumor targeting. However, the thermal-to-epithermal neutron flux ratio (0.43) remained above the threshold value recommended by the IAEA (≤ 0.05). In conclusion, while the collimator design was capable of delivering a high-quality epithermal neutron beam that selectively targeted the tumor, further optimization of the filter components remains necessary to reduce unwanted thermal flux and enhance therapeutic safety and efficacy.

© 2025 Atom Indonesia. All rights reserved

INTRODUCTION

Rhabdomyosarcoma (RMS) is a high-grade malignant neoplasm characterized by myogenic differentiation of tumor cells, which may arise in various anatomical sites [1]. This tumor originates from immature skeletal muscle, with the head and neck being the most frequent sites [2]. RMS accounts for 4.5% of all childhood cancers, with an incidence of approximately 4.5 cases per million children [3]. It has a median age of onset of five years, and about 70% of cases are diagnosed before the age of 10 [4].

Boron Neutron Capture Therapy (BNCT) is a form of radiotherapy that combines a neutron beam with a boron-containing compound that selectively accumulates in cancer cells [5]. The absorption of neutrons by boron-10 nuclei induces an immediate nuclear reaction, $^{10}\text{B}(n,\alpha)^7\text{Li}$, releasing an energy deposition of 2.79 MeV [6]. BNCT is distinguished by its high biological effectiveness, precise tumor targeting, minimal damage to surrounding healthy tissue, and shorter treatment duration [7]. These advantages stem from BNCT's unique ability to selectively eradicate cancer cells while sparing the surrounding healthy tissue [3]. An important advantage of BNCT over conventional radiotherapy is the markedly reduced number of treatment fractions, typically 1-3, compared to approximately

*Corresponding author.

E-mail address: fajararianto@fisika.fsm.undip.ac.id

DOI: <https://doi.org/10.55981/aij.2025.1708>

30 fractions in conventional radiotherapy [8]. Furthermore, BNCT has demonstrated encouraging results in locally recurrent tumors, including those of the central nervous system and head and neck [9]. BNCT is considered a suitable therapeutic modality for pediatric head and neck cancers, offering low toxicity and high tumor response rates [10].

The neutrons generated in BNCT are classified into thermal, epithermal, and fast energy ranges [11]. For therapeutic purposes, BNCT primarily utilizes epithermal neutrons (0.5 eV-10 keV), which are typically generated in nuclear fission reactors [12]. The preference for epithermal neutrons arises from the limited penetration depth of thermal neutrons, which leads to insufficient doses for effectively treating deep-seated tumors [13]. Neutron flux is defined as the number of neutrons crossing an area of 1 cm² per second when traversing a medium [14].

The Monte Carlo method is a statistical technique used to simulate particle trajectories from their point of origin to termination [15]. This method relies on numerical analysis with random probabilistic sampling [16]. MCNP, one of the most widely used software packages, applies the Monte Carlo method in nuclear medicine, radiation physics, nuclear security, accelerator-based applications, and nuclear criticality studies [17].

Given the high incidence of RMS in the head and neck region of children under 10 years of age, and the growing demand for effective yet minimally invasive therapies, BNCT has emerged as a promising alternative. Its capacity to selectively target tumor cells while sparing healthy tissue makes it particularly suitable for pediatric patients, with developing tissues that are more susceptible to radiation-induced damage.

In this study, a 10-year-old pediatric model was selected to represent a typical age at which Rhabdomyosarcoma (RMS) remains prevalent, while also providing anatomical characteristics suitable for accurate dosimetric simulations. This choice was compared with the previous research by Syamputra et al. (2018), which employed a 5-year-old model, thereby expanding the understanding of BNCT applications across different pediatric age groups. Ethical approval was not required, as all procedures were carried out through simulations without the use of patient data [18].

This study aims to evaluate the neutron flux generated by the BNCT collimator through Monte Carlo simulations using the MCNP 6.2 method. The evaluation covers thermal, epithermal, and fast neutron fluxes. In BNCT, neutron flux plays a

critical role in assessing the quality of the collimator output, as a high-quality flux directly influences therapeutic effectiveness. The measured neutron flux was then compared against IAEA standards to ensure its suitability for therapeutic applications. According to the IAEA reference, neutron flux parameters serve as the primary benchmark for evaluating BNCT beam quality. Accordingly, this study focuses specifically on the analysis of neutron flux distribution [5].

METHODOLOGY

This study employed MCNP version 6.2, a Monte Carlo-based software for simulating radiation particle transport [19]. The simulation was conducted to calculate the neutron flux distribution produced by the BNCT collimator. Input codes were written in Notepad++ and executed using Total Commander (64-bit). A total of 10 million particles (10⁷ NPS) were simulated, exceeding the recommended minimum of 5,000-10,000 NPS as specified in the MCNP User Manual. This number was chosen to ensure statistically reliable results. Simulation convergence was evaluated by monitoring the ten statistical check parameters available in the output file.

The neutron cross-section library employed in this simulation was ENDF/B-VII.1, as defined in the default *xsdir* file of MCNP 6.2. This library provides the evaluated data necessary for accurately modeling neutron transport and interactions.

The BNCT collimator design was adapted from Handayani et al. (2024), with the neutron source derived from the Kartini Reactor. The collimator model comprised layered components and materials engineered to generate a neutron beam within the epithermal energy range suitable for therapeutic applications [16]. The collimator geometry was visualized using the Visual Editor (VISED) X_24E and is illustrated in Fig. 1.

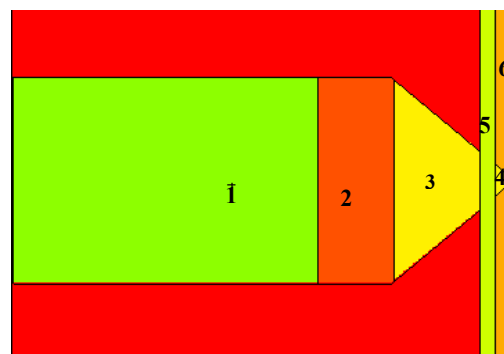


Fig. 1. Geometry of the BNCT collimator as visualized using VISED.

The collimator consists of several functional components. Component 1, an aluminum moderator with a total length of 60 cm, serves to slow down fast neutrons into epithermal and thermal energies. Component 2, a nickel filter 15 cm in length, attenuates high-energy neutrons and minimizes damage to the surrounding healthy tissues. Component 3 forms the core structure of the collimator, shaping and narrowing the beam path, while the collimator's distal end adjusts the beam size to match the treatment area. The collimator is also equipped with radiation shielding elements: Component 5 is a gamma shield made of bismuth (3 cm thick), and Component 6 is a neutron barrier made of Li_2CO_3 (3.5 cm thick), both serving to reduce unwanted radiation exposure.

The digital phantom employed in this simulation represents a 10-year-old pediatric model adapted from the ORNL-MIRD (Oak Ridge National Laboratory - Medical Internal Radiation Dose) reference. The model was modified to encompass only the head and neck region, including critical organs such as the brain, spinal cord, and thyroid gland.

The tumor was modeled as a spherical structure located in the posterior region of the brain and spinal cord, comprising three concentric treatment zones: a Gross Tumor Volume (GTV) with a diameter of 1.5 cm, a Clinical Target Volume (CTV) of 1.8 cm, and a Planning Target Volume (PTV) of 2.0 cm. According to clinical BNCT requirements, the boron-10 concentration in the tumor tissue was set at 70 $\mu\text{g/g}$.

Three types of tallies were employed to evaluate the key parameters in this simulation. Tally F4 was used to calculate neutron fluxes (thermal, epithermal, and fast) traversing the cells, Tally F24 measured the primary gamma dose rate, and Tally F34 assessed the fast neutron dose rate. The outputs from these tallies were used to evaluate beam quality according to IAEA (2023) criteria, including the therapeutic epithermal neutron flux ($\Phi_{\text{epithermal}}$), the fast neutron dose rate to epithermal neutron flux ratio ($\dot{D}_f/\Phi_{\text{epithermal}}$), the gamma dose rate to epithermal neutron flux ratio ($\dot{D}_\gamma/\Phi_{\text{epithermal}}$), and the thermal-to-epithermal neutron flux ratio ($\Phi_{\text{thermal}}/\Phi_{\text{epithermal}}$)[5]. These values were analyzed to determine the beam's compliance with clinical standards for BNCT in pediatric head and neck cancer.

RESULTS AND DISCUSSION

The simulation was performed using Total Commander 64-bit with 1.0×10^7 NPS. The statistical validity of the results was verified using the Tally Fluctuation Chart (TFC) provided in MCNP 6.2.

Based on the outputs of three tallies (F4, F24, and F34), the relative errors obtained were 0.168%, 0.632%, and 0.234%, respectively. These values are well below the 10% threshold recommended by the MCNP User's Manual. Furthermore, all three tallies exhibited high figures of merit (FOM): 1187.3 for F4, 249.1 for F24, and 706.6 for F34, indicating good statistical efficiency. Evaluation using the ten statistical check parameters outlined in the MCNP® User's Manual (LA-UR-17-29981) revealed no oscillatory trends, significant deviations, or inter-batch correlations. Therefore, the simulation results achieved both numerical convergence and statistical stability, and can be considered reliable for analyzing neutron flux and radiation dose distributions within the BNCT configuration.

The simulation generated neutron flux data from the BNCT collimator, encompassing thermal, epithermal, and fast neutrons. Additional output parameters include the fast neutron dose rate and the primary gamma dose rate, as presented in Table 1.

Compared to the findings of Handayani et al. (2024), the epithermal neutron flux in the present study exhibited a substantial increase [16]. Handayani reported an epithermal flux of $4.23 \times 10^9 \text{ n}\cdot\text{cm}^{-2}\cdot\text{s}^{-1}$ at the Gross Tumor Volume (GTV), whereas the present study obtained $1.22 \times 10^{10} \text{ n}\cdot\text{cm}^{-2}\cdot\text{s}^{-1}$ [16]. This enhancement is attributed to additional optimizations in the collimator design, including the use of a 60 cm aluminum moderator and a 15 cm nickel filter, which improved the moderation of fast neutrons into the epithermal range. Furthermore, the addition of a bismuth gamma shield and a Li_2CO_3 neutron absorber contributed to a more selective neutron energy spectrum without significantly increasing gamma or fast neutron exposure.

Table 1. Neutron flux of the BNCT collimator.

Parameter	Output	Unit
Thermal neutron flux	5.22×10^9	$\text{n cm}^{-2} \text{s}^{-1}$
Epithermal neutron flux	1.22×10^{10}	$\text{n cm}^{-2} \text{s}^{-1}$
Fast neutron flux	5.91×10^7	$\text{n cm}^{-2} \text{s}^{-1}$
Fast neutron dose rate	2.63×10^{-5}	Gy/s
Primary gamma dose rate	2.22×10^{-4}	Gy/s

Table 2. BNCT collimator beam quality parameters.

Flux Neutron Parameter	IAEA Standard	Study Result	Unit
Epithermal flux neutron ($\Phi_{epithermal}$)	$\geq 5.0 \times 10^8$	1.22×10^{10}	$\text{n cm}^{-2} \text{s}^{-1}$
Fast neutron scattering dose rate per epithermal neutron flux ($\dot{D}_f/\Phi_{epithermal}$)	$\leq 2.0 \times 10^{-13}$	1.81×10^{-14}	$\text{Gy cm}^2 \text{n}^{-1}$
Primary gamma dose rate per epithermal flux ($\dot{D}_\gamma/\Phi_{epithermal}$)	$\leq 2.0 \times 10^{-13}$	1.61×10^{-13}	$\text{Gy cm}^2 \text{n}^{-1}$
Ratio thermal neutron flux to epithermal neutron flux ($\Phi_{thermal}/\Phi_{epithermal}$)	≤ 0.05	0.43	

For the gamma dose rate, the simulation yielded a value of 2.217×10^{-4} Gy/s, which remains within the safe range and is lower than the average gamma dose reported by Handayani (3.12×10^{-4} Gy/s). This indicates that the gamma shielding configuration in the present study is more effective in reducing photon exposure without compromising the epithermal neutron flux. These parameters were subsequently compared with reference values from the IAEA (2023) to ensure compliance with BNCT beam quality standards, as summarized in Table 2 [5].

According to Table 2, the epithermal neutron flux obtained in this study was $1.22 \times 10^{10} \text{ n}\cdot\text{cm}^{-2}\cdot\text{s}^{-1}$, substantially exceeding the minimum threshold of $\geq 5.0 \times 10^8 \text{ n}\cdot\text{cm}^{-2}\cdot\text{s}^{-1}$ established by the IAEA. This result indicates that the collimator can deliver a high-intensity epithermal neutron beam, which is clinically advantageous as it correlates with shorter irradiation times and improved dose delivery efficiency, in line with the ALARA (As Low As Reasonably Achievable) principle. Compared with the previous study by Handayani et al. (2024), which employed a similar collimator design, the epithermal flux in the present study was nearly three orders of magnitude higher (from 3.11×10^7 to $1.22 \times 10^{10} \text{ n}\cdot\text{cm}^{-2}\cdot\text{s}^{-1}$), reflecting a significant enhancement in neutron moderation and transport performance despite comparable geometric configurations [16].

For the protection of healthy tissues, the fast neutron dose per epithermal flux was found to be $1.61 \times 10^{-13} \text{ Gy}\cdot\text{cm}^2\cdot\text{n}^{-1}$, remaining within the IAEA limit of $\leq 2.0 \times 10^{-13} \text{ Gy}\cdot\text{cm}^2\cdot\text{n}^{-1}$. This indicates that the system successfully moderated fast neutrons into a therapeutically safe energy range. Similarly, the primary gamma dose per epithermal flux was recorded at $1.81 \times 10^{-14} \text{ Gy}\cdot\text{cm}^2\cdot\text{n}^{-1}$, well below the IAEA limit, demonstrating the effectiveness of the bismuth shielding in minimizing photon radiation exposure.

Nevertheless, a challenge arises with the thermal-to-epithermal neutron flux ratio, calculated at 0.43, well above the IAEA threshold of ≤ 0.05 . This indicates that, despite the significant enhancement in epithermal flux, a substantial fraction is still converted

into thermal neutrons, possibly due to secondary interactions within biological media or inefficiencies in the thermal neutron filtering system. For comparison, Handayani et al. reported a thermal-to-epithermal ratio of 0.077, which, although still above the threshold, is lower than the value observed in the present study [16]. These findings underscore the need for further optimization of filter thickness, composition, and internal collimator material distribution to minimize the presence of undesired thermal neutrons.

The directed neutron beam reaching the target comprises a heterogeneous mixture of thermal, epithermal, and fast neutrons. Consequently, the flux distribution across organs was analyzed. The study generated a neutron flux versus organ plot, as shown in Fig. 2.

The simulation results indicate that the highest epithermal neutron flux occurred in the GTV (Gross Tumor Volume), the primary site of Head and Neck Rhabdomyosarcoma (HNRMS). The predominance of epithermal flux in the GTV demonstrates the collimator's effectiveness in selectively directing epithermal neutrons toward the tumor region. This is consistent with the fundamental BNCT principle of maximizing interactions between thermal neutrons and ^{10}B atoms accumulated in cancer cells. Epithermal neutrons are crucial for penetrating superficial tissues and being moderated into thermal neutrons near the tumor site, thereby facilitating effective $^{10}\text{B}(\text{n},\alpha)^7\text{Li}$ reactions within the target volume.

The neutron flux in healthy organs, including the brain, spinal cord, and thyroid, was significantly lower than that in the GTV. This indicates a favorable selectivity gradient for therapeutic purposes. The neutron beam was not uniformly distributed but rather concentrated at the target site. Importantly, the consistently low fast neutron flux across all organs underscores the effectiveness of the collimator system in minimizing potential damage to healthy tissues from high-energy particles.

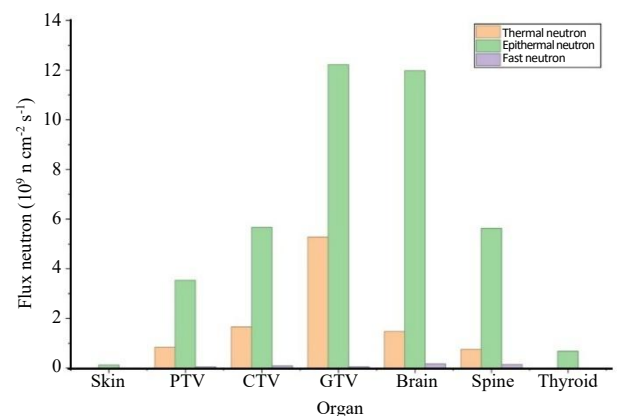


Fig. 2. Graph of neutron flux for each organ in the head and neck phantom.

This flux distribution pattern is consistent with the findings of Handayani et al. (2024), who employed a similar collimator design for lung cancer cases with a boron dose of 60 $\mu\text{g/g}$. That study likewise reported the highest neutron flux in the GTV compared to the surrounding healthy lung tissue [16]. Despite differences in tumor location, cancer type, and boron concentration, this consistent spatial pattern confirms the effectiveness of the collimator design in producing a directed neutron beam. These findings further strengthen the geometric validity of the collimator model used in the present study.

A key difference lies in the absolute neutron flux values observed at the GTV and surrounding tissues. The higher flux values in the present study are likely influenced by anatomical differences between the head and neck region and the lungs, particularly in terms of tissue density and structure. Nevertheless, the spatial flux characteristics remain consistent in both studies, high at the GTV and decreasing in healthy organs. This finding confirms that the collimator system can efficiently direct neutrons to the therapeutic target while reducing exposure to non-target tissues, which is a critical criterion in BNCT-based radiotherapy.

In conclusion, this study demonstrates superior performance in terms of epithermal neutron beam intensity and quality, while also highlighting the need for further optimization to address the excessive thermal component. The analysis not only confirms the numerical and statistical reliability of the simulation but also provides a strong physical basis for the development of a more selective and efficient BNCT system.

CONCLUSION

From this study, it can be concluded that the neutron flux values obtained were $5.22 \times 10^9 \text{ n}\cdot\text{cm}^{-2}\cdot\text{s}^{-1}$ for thermal neutrons, $1.22 \times 10^{10} \text{ n}\cdot\text{cm}^{-2}\cdot\text{s}^{-1}$ for epithermal neutrons, and $5.91 \times 10^7 \text{ n}\cdot\text{cm}^{-2}\cdot\text{s}^{-1}$ for fast neutrons, with one test parameter unmet concerning the ratio of thermal to epithermal neutron flux. The calculated ratio of 0.43 is substantially higher than the IAEA's recommended limit of ≤ 0.05 . These findings indicate the need for further research, particularly focusing on optimizing the material composition and thickness of the filter, to effectively suppress the undesired thermal neutron component and improve the overall quality of the therapeutic beam.

ACKNOWLEDGMENT

The author would like to thank the Dean of the Faculty of Science and Mathematics, Diponegoro University, for supporting this work through a mid-level research grant.

AUTHOR CONTRIBUTION

The first author was responsible for conducting the main research and drafting the manuscript. The second and third authors provided supervision and theoretical validation. The fourth author contributed to the design of the research methodology and administrative coordination.

REFERENCES

1. K. P. D. Gallagher, A. L. O. C. Roza, E. M. J. R. Tager *et al.*, Head Neck Pathol. **17** (2023) 546.
2. C. Chen, H. D. Garcia, M. Scheer *et al.*, Front. Oncol. **9** (2019) 1458.
3. H. Kumada, T. Sakae, and H. Sakurai, EPJ Tech. Instrum. **10** (2023) 18.
4. S. Y. Taskaev, Phys. At. Nucl. **84** (2021) 207.
5. IAEA, Advances in Boron Neutron Capture Therapy, International Atomic Energy Agency, Vienna (2023) 1.
6. F. Naito, Ther. Radiol. Oncol. **2** (2018) 1.
7. Z. Huanyu, Z. Pengcheng, Z. Youzhe *et al.*, Chin. J. Radiat. Oncol. **32** (2023) 848.
8. T. Murakami, M. Hamada, K. Odagiri *et al.*, Tokai J. Exp. Clin. Med. **47** (2022) 85.
9. Z. Liu, W. Cheng, W. Wu *et al.*, Med. J. Peking Union Med. Coll. Hosp. **14** (2023) 698.
10. Y. W. Chen, T. L. Lan, Y. Y. Lee *et al.*, Ther. Radiol. Oncol. **4** (2020) 1.
11. M. Suzuki, Int. J. Clin. Oncol. **25** (2020) 43.
12. E. Ratnawati, J. Iman and H. Ali, Buletin Pengelolaan Reaktor Nuklir **13** (2017) 19. (in Indonesian)
13. R. A. D. S. T. K. Wardani and Suharyana, Jurnal Fisika **13** (2023) 40. (in Indonesian)
14. R. D. Putra, Y. Apridiansyah, and E. Sahputra, Processor: Jurnal Ilmiah Sistem Informasi, Teknologi Informasi dan Sistem Komputer **17** (2022) 74. (in Indonesian)

15. H. O. Tekin and U. Kara, J. Commun. Comput. **13** (2016) 32.
16. N. Handayani, K. K. Soelistiyono, and F. Arianto, Indones. J. Appl. Phys. **14** (2024) 176.
17. T. Nishitani, S. Yoshihashi, Y. Tanagami *et al.*, J. Nucl. Eng. **3** (2022) 222.
18. D. N. I. Syamputra, Y. Sardjono and R. S. N. Mahmudah, ASEAN J. Sci. Technol. Dev. **35** (2018) 235.
19. B. El Azzaoui, O. Kabach, R. Outayad *et al.*, Atom Indones. **50** (2024) 231.